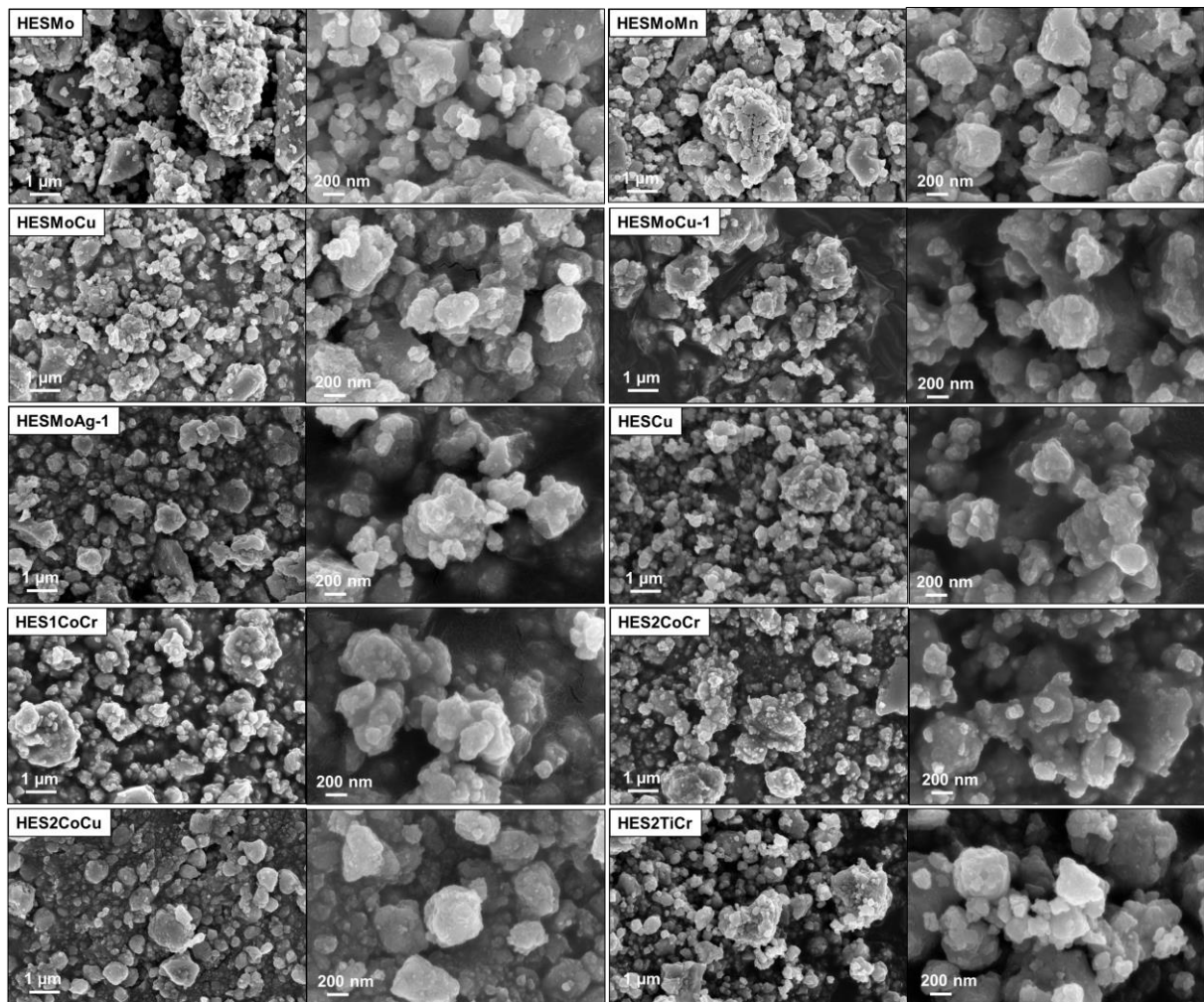


# Supporting Information

## High-entropy sulfides as highly effective catalysts for the oxygen evolution reaction

Ling Lin, Ziming Ding, Guruprakash Karkera, Thomas Diemant, Mohana Veerraju Kante, Daisy Agrawal, Horst Hahn, Jasmin Aghassi, Maximilian Fichtner, Ben Breitung\* and Simon Schweidler\*



**Figure S1.** Exemplary top-view SEM images of HESs

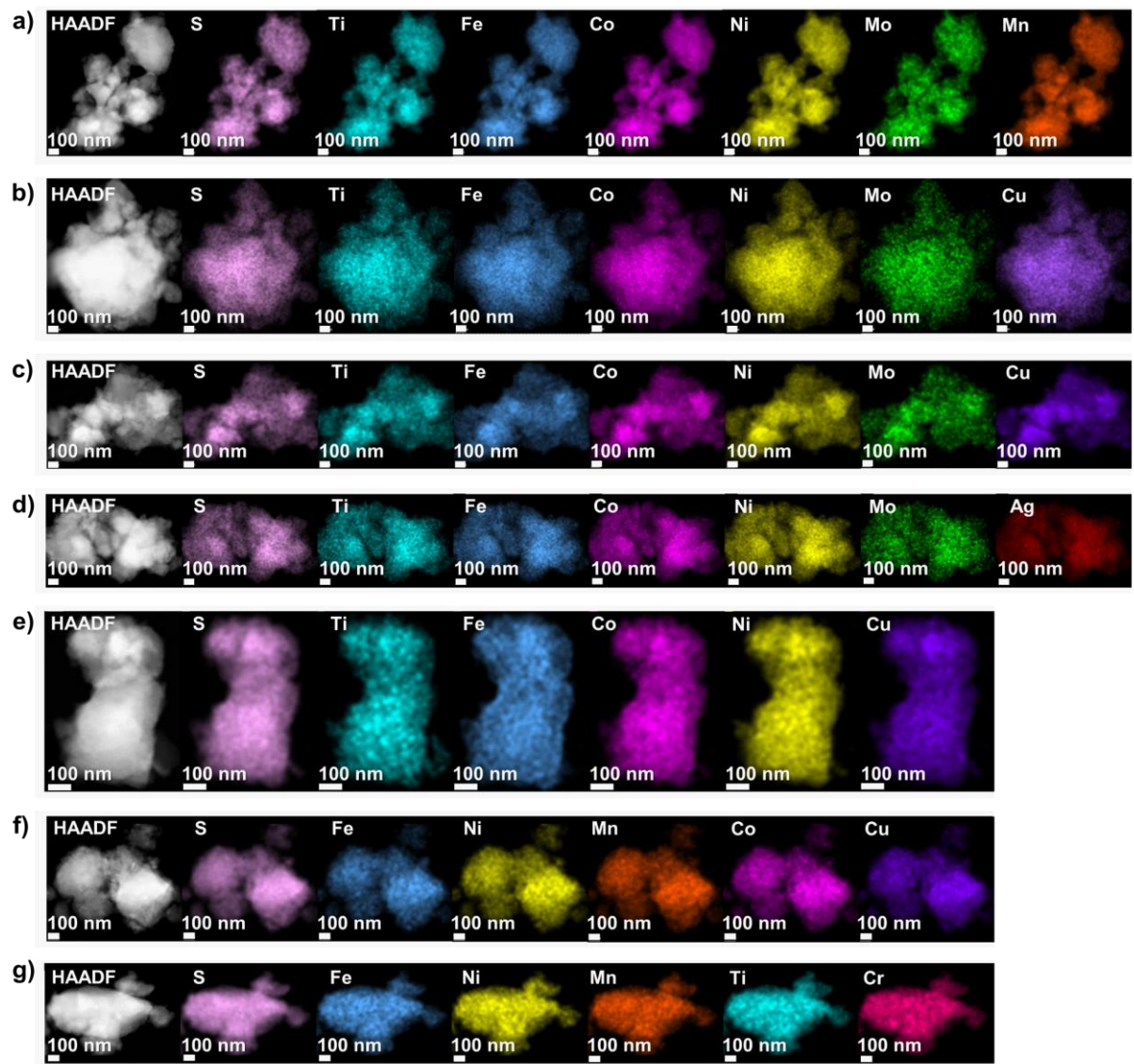


**Figure S2.** STEM-EDX mapping of a) HESMoMn, b) HESMoCu, c) HESMoCu-1, d) HESMoAg-1, e) HESCu, f) HES2CoCu, g) HES2TiCr.

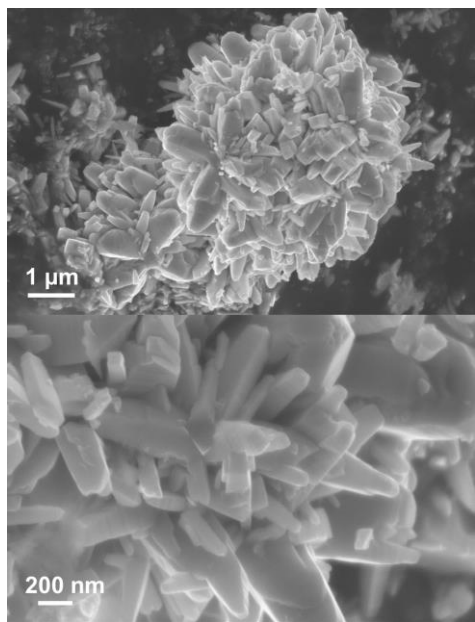


**Figure S3.** Exemplary top-view SEM image of  $\text{IrO}_2$

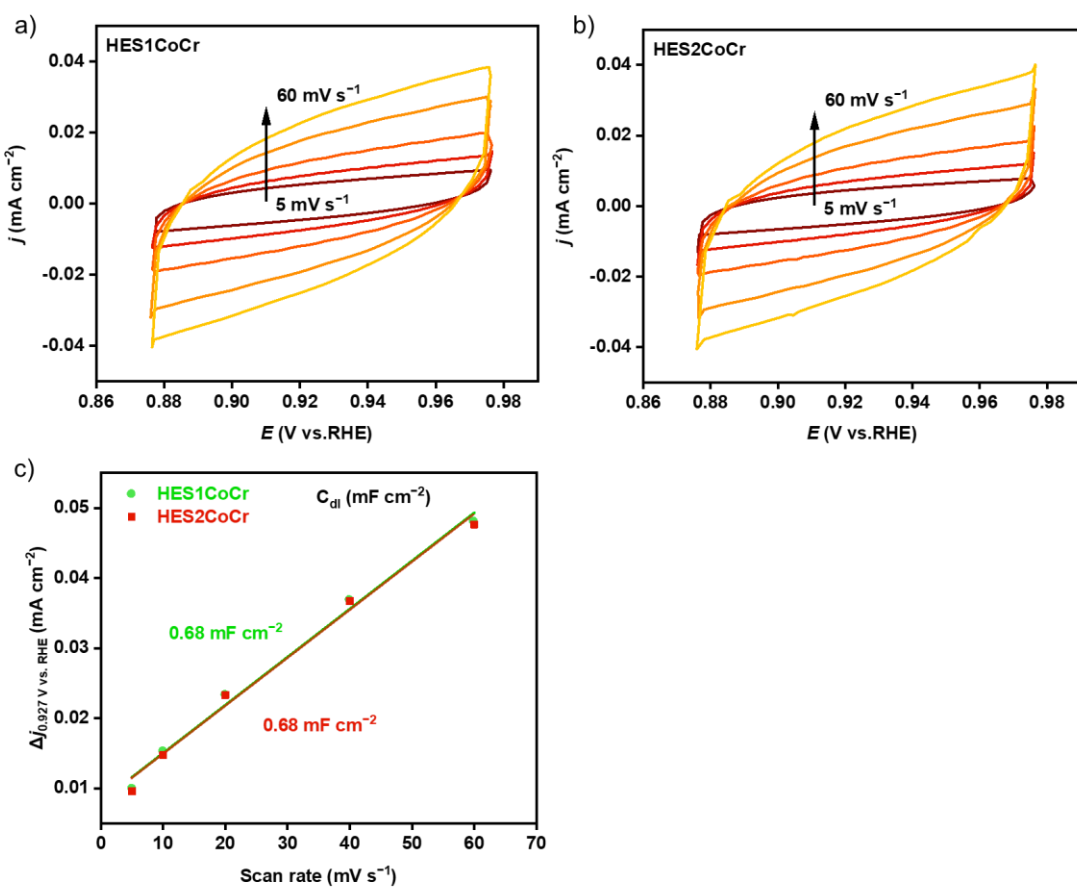


**Figure S4.** CV curves at different scan rates (5, 10, 20, 40, and 60 mV s<sup>-1</sup>) of a) HES1CoCr and b) HES2CoCr. c) Current density differences ( $\Delta j$ ) of HES1CoCr and HES2CoCr from CV curves plotted against the scan rate. The  $C_{dl}$  can be determined from the linear slope.

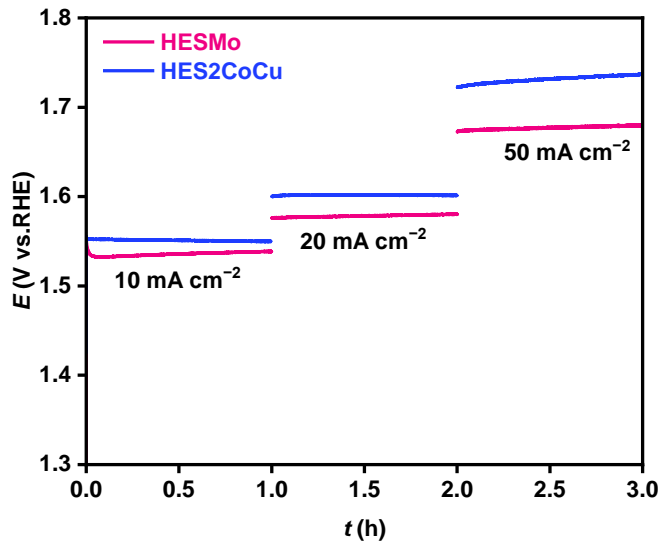


**Figure S5.** Multi-step chronopotentiometry of HESMo and HES2CoCu at current densities of 10, 20 and 50 mA cm<sup>-2</sup>.

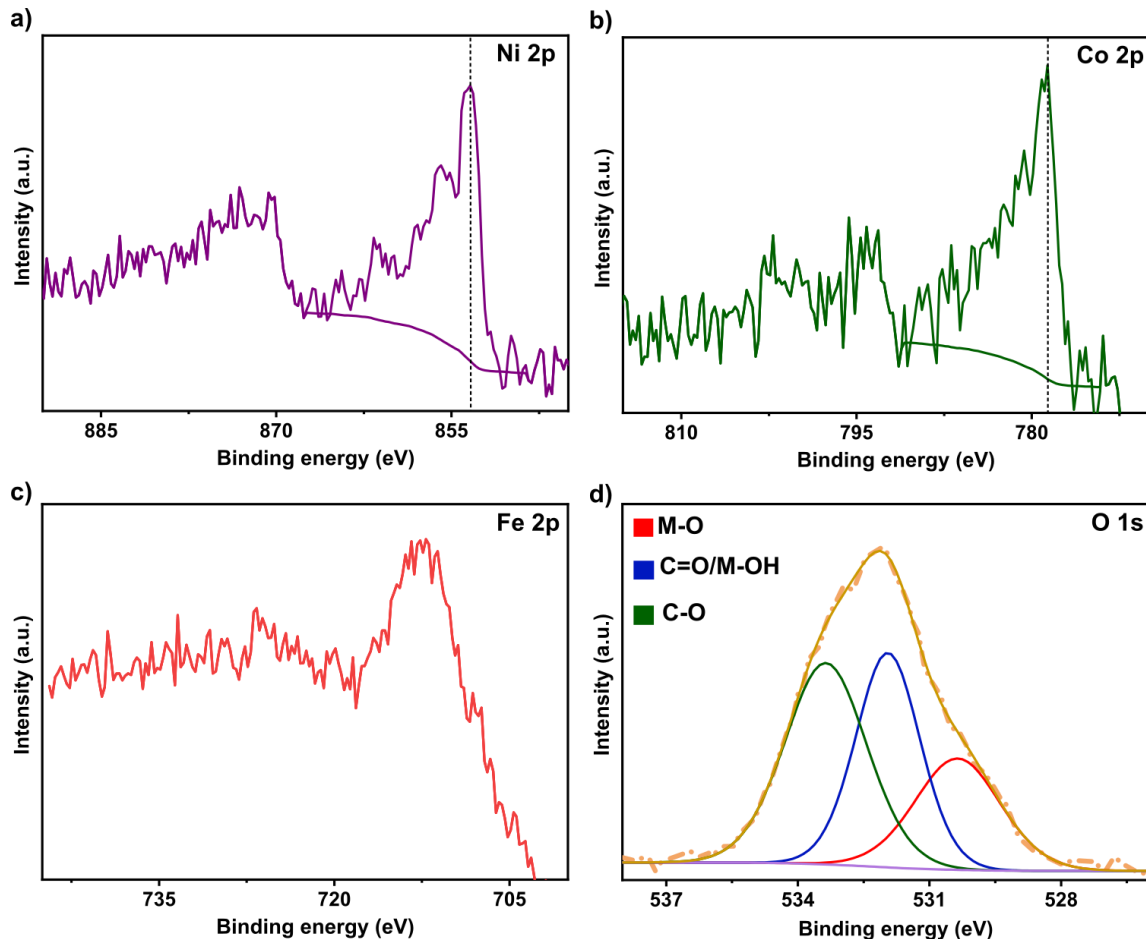


**Figure S6.** XPS detail spectra of HESMo in the a) Ni 2p, b) Co 2p, c) Fe 2p and d) O 1s region.

**Table S1.** Stoichiometry of HESs from ICP-OES and EDX analysis.

Materials	Method	Mass ratio [%]
HESMo	Expected value	Ti 5.5 Fe 12.8 Co 13.5 Ni 20.2 Mo 11.0 S 36.9
	ICP-OES	Ti 5.6 Fe 13.3 Co 13.6 Ni 19.8 Mo 10.2 S 28.5 undefined part 9.0
	EDX	Ti 5.2 Fe 12.2 Co 12.9 Ni 17.9 Mo 9.0 S 42.7
HESMoMn	Expected value	Ti 4.6 Mn 10.5 Fe 10.7 Co 11.3 Ni 16.9 Mo 9.2 S 36.9
	ICP-OES	Ti 4.7 Mn 10.7 Fe 12.0 Co 12.2 Ni 17.1 Mo 8.6 S 31.4 undefined part 3.3
	EDX	Ti 4.8 Mn 11.0 Fe 11.4 Co 12.0 Ni 16.5 Mo 9.0 S 35.2
HESMoCu	Expected value	Ti 4.5 Fe 10.5 Co 11.1 Ni 16.6 Cu 12.0 Mo 9.0 S 36.3
	ICP-OES	Ti 4.2 Fe 11.4 Co 12.1 Ni 17.4 Cu 13.3 Mo 8.9 S 32.4 undefined part 0.3
	EDX	Ti 4.6 Fe 10.0 Co 10.8 Ni 14.8 Cu 11.9 Mo 8.2 S 39.8
HESMoCu-1	Expected value	Ti 4.7 Fe 10.9 Co 11.4 Ni 17.1 Cu 12.3 Mo 9.3 S 34.3
	ICP-OES	Ti 4.8 Fe 11.3 Co 11.7 Ni 17.0 Cu 12.7 Mo 8.7 S 33.6 undefined part 0.2
	EDX	Ti 4.5 Fe 10.2 Co 10.6 Ni 14.7 Cu 14.8 Mo 8.3 S 36.9
HESMoAg-1	Expected value	Ti 4.3 Fe 10.0 Co 10.5 Ni 15.8 Mo 8.6 Ag 19.3 S 31.5

	ICP-OES	Ti 4.5 Fe 10.1 Co 10.2 Ni 16.0 Mo 7.8 Ag 0.7 S 27.7 undefined part 23.0
	EDX	Ti 4.5 Fe 9.8 Co 10.2 Ni 14.9 Mo 8.2 Ag 16.1 S 36.2
HESCu	Expected value	Ti 5.3 Fe 12.4 Co 13.1 Ni 19.5 Cu 14.1 S 35.6
	ICP-OES	Ti 5.0 Fe 11.7 Co 12.3 Ni 17.4 Cu 14.5 S 17.8 undefined part 21.3
	EDX	Ti 5.2 Fe 11.1 Co 12.2 Ni 16.4 Cu 16.6 S 38.6

The expected values are calculated using the synthetic compositions listed in **Table 1**. The measurement results are largely in line with expectations. Although the Ag content of HESMoAg-1 and some S contents determined by ICP-OES are lower than expected, these missing contents are probably contained in an undefined part, such as undetectable precipitates insoluble in aqua regia. When further analyzed by combining the EDX results, the ratios of the elements are essentially close to the expected values.

**Table S2.** Comparison of OER performance among HESMoMn and some reported transition metal sulfides or derivatives with glassy carbon working electrode in alkaline media.

Catalysts	Overpotential [mV] @10 mA cm <sup>-2</sup>	Tafel slope [mV dec <sup>-1</sup> ]	Reference
TiFe <sub>2</sub> Co <sub>2</sub> Ni <sub>3</sub> MoMn <sub>2</sub> S <sub>12</sub>	288	43.6	This work
hierarchical porous Ni <sub>3</sub> S <sub>4</sub>	307	67	[1]
CoS/CNT composite	330	142	[2]
Mo–N/C@MoS <sub>2</sub>	390	72	[3]
3% Ni-doped CuS	390	96.8	[4]
CuCo <sub>2</sub> S <sub>4</sub> nanosheets	310	86	[5]
Ni <sub>1.29</sub> Co <sub>1.49</sub> Mn <sub>0.22</sub> S <sub>4</sub>	348	65	[6]
Co <sub>1-x</sub> Ni <sub>x</sub> S <sub>2</sub> –graphene composite	330	47	[7]
FeNiS <sub>2</sub> nanosheets	310	46	[8]
Ti–Fe mixed sulfide nanoboxes	350	55	[9]

**Table S3.** Summary of effects on catalytic performance.

Abbreviation	Composition	Structure	Effect on OER performance
HESMo	TiFe <sub>2</sub> Co <sub>2</sub> Ni <sub>3</sub> MoS <sub>10</sub>	<i>Pnma</i>	The catalytic OER performance can be improved by incorporating Mo into the multi-metal high entropy system.
HESMoMn	TiFe <sub>2</sub> Co <sub>2</sub> Ni <sub>3</sub> MoMn <sub>2</sub> S <sub>12</sub>	<i>Pnma</i>	The introduction of Mn slightly reduces the overpotential.
HESMoCu	TiFe <sub>2</sub> Co <sub>2</sub> Ni <sub>3</sub> MoCu <sub>2</sub> S <sub>12</sub>	<i>Pnma</i>	Compared with HESCu, the overpotential is greatly reduced by introducing Mo.

HESMoCu-1	TiFe <sub>2</sub> Co <sub>2</sub> Ni <sub>3</sub> MoCu <sub>2</sub> S <sub>11</sub>	<i>Pnma</i>	Compared with HESMoCu, changing Cu precursor from CuS (Cu <sup>2+</sup> ) to Cu <sub>2</sub> S (Cu <sup>1+</sup> ) results in a significant increase in overpotential.
HESMoAg-1	TiFe <sub>2</sub> Co <sub>2</sub> Ni <sub>3</sub> MoAg <sub>2</sub> S <sub>11</sub>	<i>Pnma</i>	Similar poor OER performance is observed for HESMoAg-1 and HESMoCu-1. Incorporation of the +1 metal cations Cu or Ag leads to a significant deterioration of the OER activity, which may be due to the lack of formation of efficient catalytically active species of these metal ions.
HESCu	TiFe <sub>2</sub> Co <sub>2</sub> Ni <sub>3</sub> Cu <sub>2</sub> S <sub>10</sub>	<i>Pnma</i>	Compared with HESMo, the overpotential is clearly increased by replacement of Mo by Cu.
HES1CoCr	MnFeNiCoCrS <sub>5</sub>	<i>Pnma</i>	HES1CoCr (M:S = 1:1) shows a bit better OER activity than HES2CoCr (M:S = 1:2), which could be attributed to the higher proportion of cations.
HES2CoCr	MnFeNiCoCrS <sub>10</sub>	<i>Pa-3</i>	Crystal structures (Pa-3 and Pnma) of the nanoparticles hardly affect the ECSA.
HES2CoCu	MnFeNiCoCuS <sub>10</sub>	<i>Pa-3</i>	Replacing Cr with Cu causes very slight reduction in overpotential.
HES2TiCr	MnFeNiTiCrS <sub>10</sub>	<i>Pa-3</i>	Replacing Co with Ti results in relatively higher overpotential, possibly due to stronger synergistic effect between other transition metals and Co than Ti.

## References

- [1] K. Wan, J. Luo, C. Zhou, T. Zhang, J. Arbiol, X. Lu, B. W. Mao, X. Zhang, J. Fransaer, *Adv. Funct. Mater.* **2019**, *29*, 1900315.
- [2] K. Prabakaran, M. Lokanathan, B. Kakade, *Appl. Surf. Sci.* **2019**, *466*, 830.
- [3] I. S. Amiinu, Z. Pu, X. Liu, K. A. Owusu, H. G. R. Monestel, F. O. Boakye, H. Zhang, S. Mu, *Adv. Funct. Mater.* **2017**, *27*, 1702300
- [4] J. Kundu, S. Khilari, K. Bhunia, D. Pradhan, *Catal. Sci. Technol.* **2019**, *9*, 406.
- [5] M. Chauhan, K. P. Reddy, C. S. Gopinath, S. Deka, *ACS Catal.* **2017**, *7*, 5871.
- [6] Y. Xu, A. Sumboja, A. Groves, T. Ashton, Y. Zong, J. A. Darr, *RSC Adv.* **2020**, *10*, 41871.
- [7] H. Han, K. M. Kim, H. Choi, G. Ali, K. Y. Chung, Y. R. Hong, J. Choi, J. Kwon, S. W. Lee, J. W. Lee, J. H. Ryu, T. Song, S. Mhin, *ACS Catal.* **2018**, *8*, 4091.
- [8] J. Jiang, S. Lu, H. Gao, X. Zhang, H. Q. Yu, *Nano Energy* **2016**, *27*, 526.
- [9] J. W. Nai, Y. Lu, X. Y. Yu, *J. Mater. Chem. A* **2018**, *6*, 21891.